



## Disruptive 3D *in vitro* models for respiratory disease investigation: A state-of-the-art approach focused on SARS-CoV-2 infection

Maria Luiza Seixas<sup>a</sup>, Cynthia Silva Bartolomeo<sup>a,b</sup>, Robertha Lemes<sup>c,d</sup>, Tiago Nicoliche<sup>a</sup>, Liria Hiromi Okuda<sup>e</sup>, Leonardo Martins<sup>f</sup>, Rodrigo Ureshino<sup>c,d,g</sup>, Carla Maximo Prado<sup>b</sup>, Tácia Tavares Aquinas Liguori<sup>h</sup>, Gabriel Romero Liguori<sup>h</sup>, Roberta Sessa Stilhano<sup>a,g,\*</sup>

<sup>a</sup> Department of Physiological Sciences, Santa Casa de São Paulo School of Medical Sciences, São Paulo, Brazil

<sup>b</sup> Department of Biosciences, Federal University of São Paulo, Santos, Brazil

<sup>c</sup> Department of Biological Sciences, Federal University of São Paulo, Diadema, Brazil

<sup>d</sup> Laboratory of Molecular and Translational Endocrinology, Federal University of São Paulo, São Paulo, SP, Brazil

<sup>e</sup> Biological Institute, Agriculture and Supply Department, São Paulo, SP, Brazil

<sup>f</sup> Division of Medical Sciences, Laboratory of Transcriptional Regulation, Institute of Medical Biology of Polish Academy of Sciences (IMB-PAN), Poland

<sup>g</sup> Post-graduation Program in Chemistry-Biology, Federal University of São Paulo, Diadema, Brazil

<sup>h</sup> TissueLabs Sagl, Manno, Switzerland

### ARTICLE INFO

#### Keywords:

SARS-CoV-2

ACE2

3D culture

COVID-19

Respiratory diseases

MatriWell

### ABSTRACT

COVID-19, along with most respiratory diseases in the medical field, demonstrates significant ability to take its toll on global population. There is a particular difficulty in studying these conditions, which stems especially from the short supply of *in vitro* models for detailed investigation, the specific therapeutic knowledge required for disease scrutinization and the occasional need of BSL-3 [Biosafety Level 3] laboratories for research. Based on this, the process of drug development is hampered to a great extent. In the scenario of COVID-19, this difficulty is even more substantial on account of the current undefinition regarding the exact role of the ACE2 [Angiotensin-converting enzyme 2] receptor upon SARS-CoV-2 kinetics in human cells and the great level of demand in the investigation process of ACE2, which usually requires the laborious and ethically complicated usage of transgenic animal models overexpressing the receptor. Moreover, the rapid progression of the aforementioned diseases, especially COVID-19, poses a crucial necessity for adequate therapeutic solutions emergence. In this context, the work herein presented introduces a groundbreaking set of 3D models, namely spheroids and MatriWell cell culture inserts, whose remarkable ability to mimic the *in vivo* environment makes them highly suitable for respiratory diseases investigation, particularly SARS-CoV-2 infection. Using MatriWells, we developed an innovative platform for COVID-19 research: a pulmonary air-liquid interface [ALI] associated with endothelial (HUVEC) cells. Infection studies revealed that pulmonary (BEAS-2B) cells in the ALI reached peak viral load at 24h and endothelial cells, at 48h, demonstrating lung viral replication and subsequent hematogenous dissemination, which provides us with a unique and realistic framework for studying COVID-19. Simultaneously, the spheroids were used to address the understudied ACE2 receptor, aiming at a pronounced process of COVID-19 investigation. ACE2 expression not only increased spheroid diameter by 20% ( $p < 0.001$ ) and volume by 60% ( $p \leq 0.0001$ ) but also led to a remarkable 640-fold increase in intracellular viral load ( $p \leq 0.01$ ). The previously mentioned finding supports ACE2 as a potential target for COVID-19 treatment. Lastly, we observed a higher viral load in the MatriWells compared to spheroids (150-fold,  $p < 0.0001$ ), suggesting the MatriWells as a more appropriate approach for COVID-19 investigation. By establishing an advanced method for respiratory tract conditions research, this work paves the way toward an efficacious process of drug development, contributing to a change in the course of respiratory diseases such as COVID-19.

\* Corresponding author at: 61 Dr. Cesário Mota Junior street, São Paulo, 01221-020, SP, Brazil.

E-mail address: [Roberta.yamaguchi@fmsantacasasp.edu.br](mailto:Roberta.yamaguchi@fmsantacasasp.edu.br) (R.S. Stilhano).

## Introduction

Coronavirus disease 2019 [COVID-19], the disease that has been declared a worldwide pandemic by the World Health Organization [WHO] on March 11<sup>th</sup>, 2020 [1], has already caused over 650 million cases and 6 million deaths as of February 2023 [2]. The virus' wide range of transmission modes (direct contact and airborne transmission) [3] facilitated its accelerated spread across the world. The disease primarily affects the respiratory tract, causing severe pneumonia, which further leads to acute respiratory distress syndrome [ARDS] [4]. Attention has also been given to extrapulmonary manifestations, such as thrombosis, arrhythmias, acute kidney injury, anorexia and diarrhea, whose emergence have progressively increased [5].

The harm to the human organism starts with viral entrance into the human cells, which takes place via SARS-CoV-2 cell surface or endosomal [6] entry. Initially, SARS-CoV-2 spike protein, which is formed by 2 subunits (S1 and S2) interacts with human ACE2. The interaction induces a conformational change in the spike protein, exposing a cleavage site between S1 and S2 [7]. This site is then cleaved either by furin followed by TMPRSS2 [Transmembrane serine protease 2] (cell surface entry) or by cathepsins (endosomal entry) when cells either express insufficient TMPRSS2 or virus-ACE2 complex does not reach TMPRSS2. Membrane fusion between viral and cellular membranes then ensues, allowing for viral RNA release into the host cell [6].

Studies regarding respiratory diseases, especially COVID-19, are particularly challenging. This is on account of specific therapeutic knowledge that is required, scarce efficient *in vitro* models for a thorough investigation, and, in the setting of viruses, the necessity of BSL-3 [Biosafety Level 3] laboratories for any kind of experiment and investigation. Drug development for those diseases, which is already a complex process, becomes even more complicated in this scenario. Over the past forty years, scant new classes of drugs have been introduced into the healthcare market for respiratory illness treatment [8]. Exceptionally concerning SARS-CoV-2 infection, the limited *in vitro* models had their role in disease investigation proven to be essential due to the sound contribution to screening for the few promising COVID-19 drug candidates [9]. The majority of those drug candidates, despite demonstrating good treatment potential in preclinical studies, still failed later in clinical trials [10]. On top of that, the rapid evolution of respiratory diseases, especially COVID-19, has not been associated with the emergence of sufficient therapeutic solutions. Therefore, drug development for those conditions has yet to be leveraged.

As to SARS-CoV-2 infection, this process is even more intricate as a consequence of the considerable difficulty studying and current uncertainty regarding the key player of the infection in human cells: ACE2. At present, the most viable option for ACE2 investigation aiming drug development is transgenic mice overexpressing the receptor [11,12]. This poses a significant level of complication to COVID-19 studies due to the fact that animal models in the COVID-19 scenario are, besides extensively laborious, extremely complex mainly as a result of the BSL-3 laboratory usage prerequisite during the entire investigation and the ethical requirements concerning animal usage in research. Furthermore, with the latest landmark report from the National Research Council ("Toxicity Testing in the 21st Century: A Vision and a Strategy"), replacement of animal tests with relevant *in vitro* human-based test systems has been strongly recommended [13]. At the same time, although previous works in our group have demonstrated a positive influence of ACE2 upon SARS-CoV-2 kinetics in 2D cell cultures [14], 2D models imperfectly simulate the *in vivo* environment [15]. In this regard, 3D models arise as an ideal solution. 3D cultures represent an accurate technique owing to their ability to mimic the *in vivo* environment. They enable the study of the morphology and cellular organization shaped by Extracellular-Matrix [ECM] interactions [16], reproducing native cell-to-cell communications, proliferation and differentiation [17] as well as response to stimuli, protein synthesis [18] and drug metabolism [19]. Thus, they contribute to a better

comprehension of disease mechanisms as well as the discovery and development of drugs. Due to their undeniable advantages, 3D cell cultures permit bypassing the usage of animal models, constituting a much more straightforward and ethical technique. Besides that, due to these benefits, they also contribute to a solid investigation of the influence of ACE2, a potential target for COVID-19 therapies, upon viral kinetics in human cells.

Although a few research studies have developed 3D models for SARS-CoV-2 infection investigation [20–23], the tridimensional cultures focused on COVID-19 are still insufficient for thorough disease investigation and drug development. Besides that, no current 3D culture has ever correlated ACE2 expression with viral kinetics investigation nor precisely represented viral hematogenous dissemination through a pulmonary air-liquid interface [ALI] associated with endothelial cells. The present work, therefore, proposes a disruptive set of 3D models especially for SARS-CoV-2 infection investigation not only based upon ACE2 expression but also capable of reproducing the SARS-CoV-2 hematogenous propagation through specific ALI formation.

Our first tridimensional culture developed and investigated was the spheroid. Spheroids were initially selected due to their powerful and high-throughput ability to simulate *in vivo* environments in particular with regard to the interrelation of cells with the surrounding ECM. Composed of an agglomeration of cellular aggregates cultivated in an ECM-rich environment, the spheroids are especially known for boosting cell-to-cell [24] and cell-ECM interactions. The strengthened interactions contribute to adequate regulation of cell functionality (e.g., viability, stimuli responsiveness and protein secretion) [25] and hence, precise representation of the natural tissues.

To enhance the accuracy of our results specifically with respect to SARS-CoV-2 infection, a second 3D model was also utilized: the MatriWell™ cell culture inserts (from here on referred to as MatriWells). The MatriWells are a cell culture insert made of biocompatible resin and designed to offer tissue-specific microenvironments to allow the fabrication of *in vitro* 3D epithelial barriers. In the apical chamber, they contain a hydrogel with tissue-specific ECM proteins, to which cells are constantly exposed. The interaction with native ECM has been shown to guide organogenesis, homeostasis [26], cell differentiation, proliferation and stem cell programming for tissue replacement [27]. Additionally, it also directs phenotype expression [28], which makes the presence of native ECM an element that confers accuracy to generated data. Above the hydrogel (apical chamber), there is a layer of air, and beneath it, a near-liquid interface (culture medium), composing a true "air-gel interface", just like in the lungs (cells exposed to air from above and ECM + other pulmonary cells from below). We, thus, utilize an ideal model for lung tissue representation.

Under a scenario of great obstacles in the study and treatment of respiratory diseases, the present investigation introduces a cutting-edge method for respiratory tract conditions research based on 2 innovative 3D cell cultures models, spheroids and MatriWells, paving the way toward an escalating and effective process of drug development. In the context of the still problematic COVID-19 pandemic, our models also make this process of drug development exceptionally valuable. This is owing to the fact that by addressing ACE2, a compound whose exact influence upon SARS-CoV-2 kinetics is still unclear, the models represent significant potential to contribute to the limited array of therapeutic solutions directed toward COVID-19.

## Materials and methods

### Cell culture

Human lung epithelial BEAS-2B cells were kindly provided by Dr. M. Macchione (INCOR-USP) and human endothelial HUVEC cells, by Prof. Dr. Sang Won Han (UNIFESP). BEAS-2B is a human bronchial epithelial cell line, immortalized and non-tumorigenic whereas HUVEC is an endothelial cell line isolated from immortalized umbilical vein. Both

were cultured in Dulbecco's Modified Essential Medium and Ham's F-12 Medium [DMEM/F12] (Sigma-Aldrich, Germany) supplemented with 10% Fetal Bovine Serum [FBS] (charcoal stripped, Thermo Fisher Scientific, United States) and gentamicin (0,02 mg/mL) (Gentamicin sulfate, Sigma-Aldrich, Germany), denominated cDMEM. Cells were incubated at 37°C in a humidified atmosphere of 5% CO<sub>2</sub> (Panasonic MCO-170AICUV(H)L-PA incubator, Panasonic, Japan) and tested free of mycoplasma contamination.

### 2.2. ACE2 Overexpression

ACE2 gene was overexpressed in BEAS-2B through nucleofection using a nucleofector 2b device (Lonza™ Nucleofector™ Transfection 2b Device, Thermo Fisher Scientific, United States) following the manufacturer's instructions with some modifications. In brief,  $1 \times 10^6$  cells were resuspended in 100uL of Opti-MEM (Opti-MEM, Reduced Serum Medium, Thermo Fisher Scientific, United States), upon which 5ug of

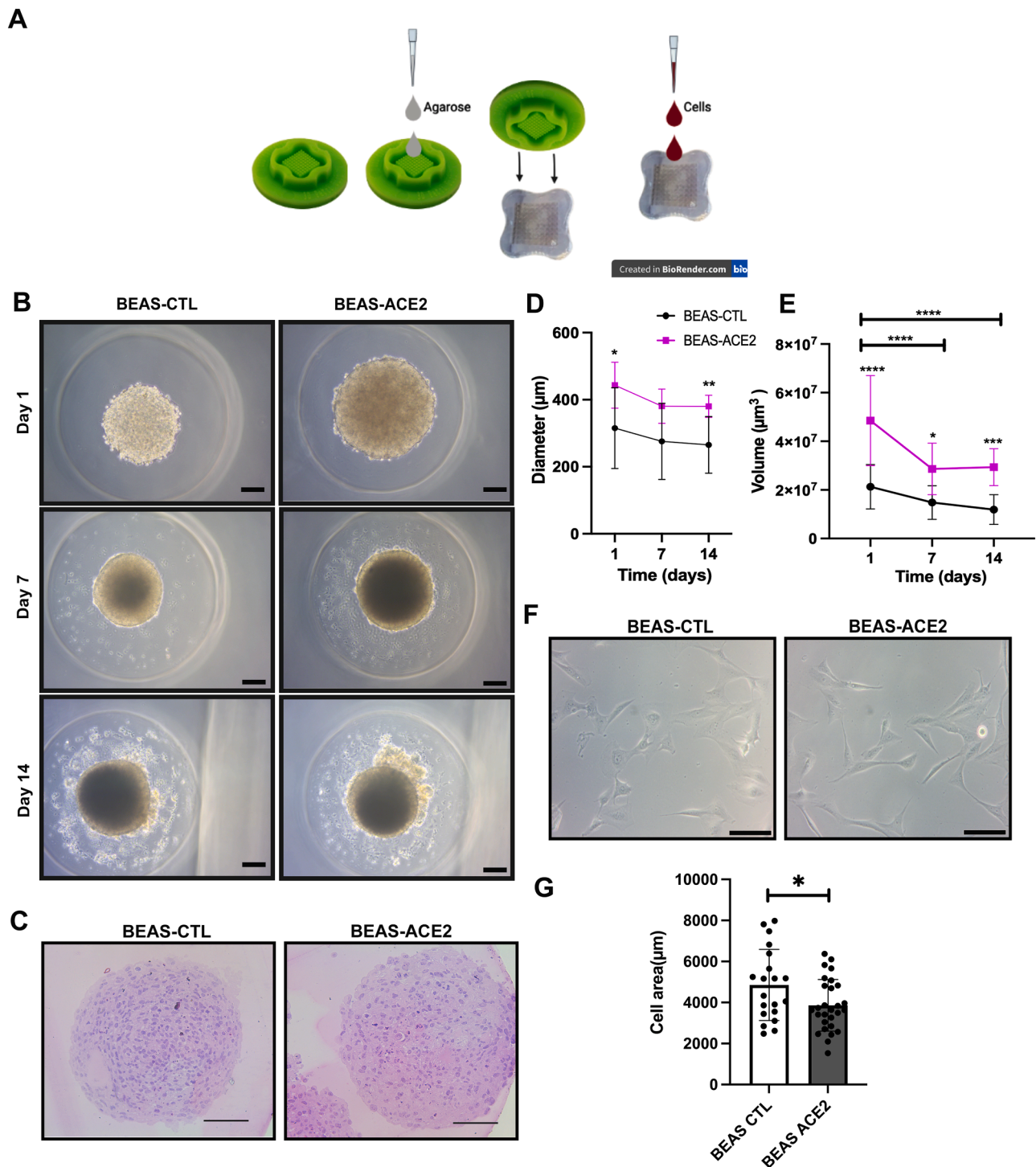


**Fig. 1. Morphological analysis and development of BEAS-CTL and BEAS-ACE2 spheroids and 2D cells.** (A) Scaffold-free spheroid-producing technique using agarose micro-molds. (B) Bright-field images of the spheroids on days 1, 7, and 14. (C) Spheroids historesin assay. Comparison of spheroids' (D) diameter and (E) volume. (F) Bright-field images of 2D cultures of BEAS-CTL and BEAS-ACE2 cells. (G) Area measurement of 2D cultures of BEAS-CTL and BEAS-ACE2 cells. Scale bar: 50-100  $\mu\text{m}$ . \* $p \leq 0.05$ ; \*\* $p \leq 0.01$ ; \*\*\*\* $p \leq 0.0001$ . n = 25-50.

pCEP4-myc-ACE2 plasmid (Addgene #141185, United States) was added and program X-001 was used for nucleofection. Afterward, cells were selected with hygromycin (60ng/mL) (Hygromycin B, Thermo Fisher Scientific, United States) for 15 days. ACE2 was also overexpressed through lentiviral transduction using pLENTI hACE2 HygR plasmid (Addgene #161758, United States). Lentiviral production and transduction were performed as previously published by Stilhano et al. [29].

### 2.3. Spheroid formation

BEAS-CTL and BEAS-ACE2 [ACE2-overexpressed-BEAS] cells were utilized for the development of spheroids, which followed a scaffold-free technique based on Stuart et al. protocol [30]. BEAS-CTL or BEAS-ACE2 ( $1 \times 10^6$  cells) were trypsinized and resuspended in 120 $\mu$ L of cDMEM and further dripped upon agarose micro-molds (Fig. 1A). The molds were maintained inside the incubator for 40 minutes. Then, 2mL of cDMEM was added to them.

Spheroids were evaluated for 14 days. Bright-field images of the spheroids were taken on days 1, 7 and 14 in ZEISS Axio Vert.A1 microscope (Germany). Spheroid had their radius, volume, and area measured using ImageJ software (radius – “Straight, segmented or freehand lines” tool, area – “Freehand selections” tool, volume –  $4\pi$  (radius)<sup>3</sup>/3) (Rasband, W.S., ImageJ, U. S. National Institutes of Health, Bethesda, Maryland, USA).

### Histology

Spheroids were collected from the agarose micro-molds to 1,5mL tubes and fixed in 4% paraformaldehyde [PFA]. Later, dehydration ensued following serial immersion on ethanol 50, 70, 90 e 100% at room temperature [RT]. Samples were further immersed in infiltration solution (ethanol + historesin [50mL] + dibenzoyl peroxide [powder]), placed on a rotator for 1 hour (pre-infiltration) and then for 2 hours under normal circumstances (infiltration) at RT. Subsequently, inclusion solution (2-hydroxyethyl-methacrylate + dimethyl sulfoxide) was added and samples were left overnight at RT for polymerization [31]. 12 hours later, the spheroids were embedded in mounting medium (polymethylmethacrylate + methyl methacrylate [2:1]). The blocks were cut into 2  $\mu$ m thick sections with Microm<sup>TM</sup> HM 525 Cryostat (Germany), mounted on adhesive slides and stained with hematoxylin-eosin [H&E]. Images were captured using the ZEISS Axio Vert.A1 inverted microscope (Germany), processed for export using ZEN Blue v.2.6 software (ZEISS) and quantified by ImageJ software.

### Cell viability assessment

The spheroids had their viability assessed via Trypan blue (Trypan Blue solution, Sigma-Aldrich, Germany) staining. The spheroids were washed with PBS, had 200 $\mu$ L of trypsin (Trypsin-EDTA 0.25%, phenol red, Gibco<sup>TM</sup> - Thermo Fisher Scientific, United States) followed by 300 $\mu$ L of cDMEM added, were centrifuged and then had 30 $\mu$ L of Trypan added. Cells were further counted.

### MatriWells development

MatriWells<sup>TM</sup> (detailed composition described in the Supplementary Material) cell culture inserts (TissueLabs Sagl, Manno, Switzerland) were placed on 12-well plates' wells filled with 2,5mL of cDMEM (the point where medium reaches the inferior portion of the MatriWells, which is in close contact with the hydrogel). The inserts were incubated with cDMEM for 2 hours in the incubator (37°C, 5% CO<sub>2</sub>). MatriWells were then removed from the wells with sterile tweezers, the medium was changed and they were repositioned inside the wells again. BEAS-ACE2 ( $1 \times 10^5$  cells) were added to the apical chamber of the structures, creating a lung tissue sample upon the hydrogel. Twenty-four

hours later, any culture medium in the apical chamber of the MatriWells was carefully aspirated.

### SARS-CoV-2 production

SARS-CoV-2 was kindly donated by Dr. J. P. M3dona. The strain was from a Brazilian patient (EPI\_ISL\_413016) and the sequence was deposited in GenBank (MT 126808). SARS-CoV-2 was amplified in the fourth passage in Vero E6 cells at a titer of  $5 \times 10^7$  plaque-forming units (PFU/mL) as previously described [14]. All the experiments with SARS-CoV-2 were performed in a BSL-3 laboratory in accordance with WHO recommendations and under the laboratory biosafety guidance required for the SARS-CoV-2 at the BLS3 facilities at the Biological Institute of S3o Paulo.

### SARS-CoV-2 infection

BEAS-ACE2 were plated on the MatriWell ( $1 \times 10^5$  cells/MatriWell), which was added in a 12-well plate, and HUVEC cells were plated in a 12-well plate ( $1 \times 10^5$  cells/well). After 24 hours, in a BSL-3 laboratory, BEAS-ACE2 MatriWells were transferred to the HUVEC plate, creating an environment where pulmonary cells (BEAS-ACE2) would hover over endothelial cells (HUVEC) in between culture medium. The layer of air above BEAS-ACE2 facilitated the formation of a pulmonary ALI that is closely associated with endothelial cells (Fig. 5A). This association offers a distinctive representation of SARS-CoV-2 kinetics within the human organism: it not only enables the visualization of viral replication in pulmonary epithelium but also allows for the depiction of further viral hematogenous dissemination through endothelial cells.

Upon ALI creation, SARS-CoV-2 (multiplicity of infection [MOI] = 0,2) was added to the apical chamber of the BEAS-ACE2 MatriWells. After 2 hours, excess viral fluid was removed from the apical chamber. SARS-CoV-2 remained in contact with the BEAS-ACE2 MatriWells for 2 hpi (2 hours post-infection), 24 hpi, and 48 hpi. Subsequently, the RNA from MatriWells and HUVEC was extracted using the RNAeasy Kit (Qiagen) according to the manufacturer's instructions. The solution between the well plate and the basal chamber of the BEAS-ACE2 MatriWells, considered the supernatant, was also collected and had viral RNA extracted. The MatriWells were infected (2, 24, and 48 hpi), used for viral RNA extraction, and had their supernatant collected and analyzed for viral quantification.

For spheroid viral infection, agarose micro-molds containing BEAS-CTL and BEAS-ACE2 spheroids were transported 1 day after spheroid development to a BSL-3 laboratory, where 200 $\mu$ L of virus (SARS-CoV-2, MOI = 0,2) were dripped upon the micro-molds. After 2 hours, excess viral fluid was removed from the superior part of the micro-molds and 24 hours later, spheroids were collected, centrifuged and had their RNA extracted as previously described.

### Quantitative real time PCR (RT-qPCR)

The cDNA was obtained from the extracted RNA using the High-Capacity Kit (High-Capacity cDNA Reverse Transcription Kit, Applied Biosystems<sup>TM</sup> - Thermo Fisher Scientific, United States) according to the manufacturer's instructions. Intracellular viral concentration was assessed through viral capsid gene expression (N gene)/endogenous gene expression (RNaseP gene) ratio and extracellular viral concentration (supernatant), through PFU/mL (plaque-forming units per mL) ratio. The primers and probes utilized were: N\_Sarbeco\_F1 - 5' CAC ATT GGC ACC CGC AAT C3', N\_Sarbeco\_R1 - 5' GAG GAA CGA GAA GAG GCT TG3' e N\_Sarbeco\_P1 - FAM 5' ACT TCC CTC AAG GAA CAA CAT TGC CA3'-BBQ (N gene), RNaseP Forward Primer - 5'AGA TTT GCA CCT GCG AGC G3' + RNaseP Reverse Primer - 5'GAG CGG CTG TCT CCA CAA GT3' (RNaseP gene) and FAM - 5'TTC TGA CCT GAA GGC TCT GCG CG3' - BH1-1 (RNaseP - probe gene) [14].

### Immunofluorescence assay

Spheroids infected with SARS-CoV-2 were subjected to free-floating immunofluorescence, according to the protocol described by Bergdorf et al. [32] with a few modifications. Spheroids were first collected and stored in 4% PFA for 30 minutes at 4°C. Then, they were resuspended in TBSTX (TBS [pure Tris base (Trimethamine, Bio-Rad, Brazil) + NaCl] + Triton [Triton X-100 detergent, Bio-Rad, Brazil]), and later, incubated with primary antibodies (Polyclonal Anti-Spike rabbit IgG [Anti-SARS-CoV-2 spike glycoprotein antibody – Coronavirus (ab272504), Abcam, United States] and Monoclonal Anti-ACE2 mouse IgG [ACE2 antibody (E-11) - sc-390851, Santa Cruz Animal Health, Brazil]) overnight at 4°C. Next, the sections were incubated for 1 h with the secondary antibodies (Alexa Fluor 594 Donkey Anti-Rabbit [Donkey anti-Rabbit IgG (H+L) Highly Cross-Adsorbed Secondary Antibody, Alexa Fluor™ 594, Thermo Fisher Scientific, United States] and Alexa Fluor 488 Goat Anti-Mouse [Goat anti-Mouse IgG (H+L) Cross-Adsorbed Secondary Antibody, Alexa Fluor™ 488]) at RT. Hoechst 33342 (Life Technologies – Invitrogen) at 1:1000 dilution was finally added. Spheroids were collected and mounted on adhesive slides. Images were captured using the ZEISS Axio Vert.A1 inverted microscope (Germany) and processed for export using ZEN Blue v.2.6 software (ZEISS).

The corrected total cell fluorescence (CTCF) of Spike protein and ACE2 expression was quantified by ImageJ software. CTCF was calculated as follows: Integrated Density – (Area of selected spheroid x Mean fluorescence of background readings). Spike protein and ACE2 CTCF were subsequently compared through Pearson correlation.

### Statistical analyses

Statistical analyses were conducted using GraphPad Prism 9 (GraphPad Software, Inc., San Diego, CA, USA). Data was evaluated by Student's t-test, one-way ANOVA (analysis of variance) followed by Tukey's multiple comparisons test, two-way ANOVA followed by Sidak's multiple comparisons test and Pearson correlation test.  $P \leq 0.05$  defined statistical significance in all cases.

## Results

### BEAS-CTL and BEAS-ACE2 spheroids characterization

To analyze the effect of ACE2 on spheroids' morphology, they were prepared and evaluated for 14 days (Fig. 1B). BEAS-CTL and BEAS-ACE2 spheroids presented similar shapes (Fig. 1B and C). On day 1, the diameter of BEAS-ACE2 spheroids was  $443.2 \pm 68.4 \mu\text{m}$ , 20% higher than BEAS-CTL ( $p < 0.001$ ). The size was reduced over time to  $380.1 \pm 49.7 \mu\text{m}$ , but it was still higher than BEAS-CTL ( $p < 0.0001$ ) (Fig. 1D). The same pattern was observed with regard to volume: BEAS-ACE2 were  $4.9 \pm 1.9 \times 10^7 \mu\text{m}^3$  on day one and  $2.9 \times 10^7 \pm 1.9 \times 10^6 \mu\text{m}^3$  on day 14, 60% higher than BEAS-CTL ( $p < 0.0001$ ) (Fig. 1E). For a more detailed morphological assessment of the spheroids, a historesin assay was also performed, confirming the data in the bright field images: increased size of BEAS-ACE2 spheroids in comparison with the control group (Fig. 1C). We then pondered if this result would be due to the difference in the cell's size. Thus, we next evaluated BEAS-CTL and BEAS-ACE2 areas. Interestingly, the area of BEAS-2B (2D) was 25% higher than BEAS-ACE2 ( $p < 0.05$ ) (Fig. 1F and G). These data showed that the higher diameter and volume of BEAS-ACE2 spheroids were not due to the cell surface area.

### Effect of ACE2 overexpression on spheroids' viability

To assess the influence of ACE2 on spheroids' viability, trypan staining was performed (Fig. 2). BEAS-CTL and BEAS-ACE2 spheroids revealed viability higher than 90% over 7 days. However, on day 14 the viability decreased to about 70% in both groups (Fig. 2). These data

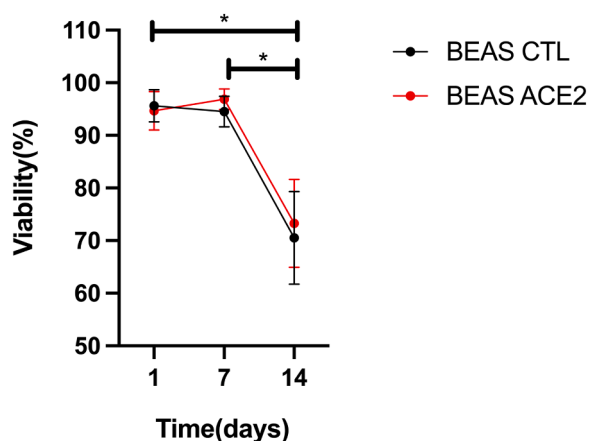


Fig. 2. BEAS-CTL and BEAS-ACE2 spheroids viability over time. The Viability over time was quantified using the trypan blue staining. \* $p \leq 0.05$ ,  $n = 3$ .

demonstrated that the overexpression of ACE2 did not influence the spheroid's viability, and the differences in the spheroids' diameter and volume were not sufficient to induce more cell death.

### Spheroids overexpressing ACE2 as a model to study SARS-CoV-2 infection

We next investigated the potential of SARS-CoV-2 to effectively enter and replicate in spheroids overexpressing ACE2. Upon infection, the intracellular viral load was 640-fold higher in BEAS-ACE2 than BEAS-CTL ( $p \leq 0.01$ ) (Fig. 3A), demonstrating that SARS-CoV-2 is able to replicate in the spheroids. Subsequently, immunofluorescence assays were performed in the infected spheroids so it would be possible to examine the extent to which SARS-CoV-2 could penetrate the spheroids and reach the center. The assay exhibited 1.7 greater ( $p \leq 0.05$ ) Spike protein expression (Fig. 3C) in the BEAS-ACE2 spheroids, which was also visibly noticed when comparing the intensity of red staining brightness on merge images from both groups (Fig. 3B) and 2 times greater ( $p \leq 0.01$ ) ACE2 expression (Fig. 3D) in the same group. A strong correlation between ACE2 expression and Spike protein staining was also observed ( $r^2 = 0.9406$ ,  $p \leq 0.0014$ ) (Fig. 3E).

### 3.4. Comparison of SARS-CoV-2 infection in spheroids and MatriWells

Having determined the positive influence of ACE2 on SARS-CoV-2 kinetics in pulmonary cells, BEAS-ACE2 cells were further employed in a model that would provide a higher accuracy level for our results: the MatriWells. Initially, the viral load in the spheroids and MatriWells were compared. For that purpose, they were infected with the same MOI of SARS-CoV-2 (MOI = 0.2), and after 24 hours the RNA was extracted and analyzed by qRT-PCR as shown in Fig. 4A. The results revealed a higher viral load (150-fold,  $p < 0.0001$ ) in BEAS-CTL seeded on the MatriWells when compared to spheroids, indicating that the Matriwell environment induced a higher viral replication (Fig. 4B). This difference was also observed when we overexpressed ACE2 in both models, in which case the viral load in the MatriWells was 4-fold higher than in the spheroids (Fig. 4C). However, the magnitude of the difference was lower than in BEAS-CTL.

### SARS-CoV-2 infection in MatriWell

Taking into account that viral replication is more efficient in the MatriWells and aiming to realistically mimic the tissue conditions of the respiratory tract, the MatriWells were utilized to develop a pulmonary ALI associated with endothelial cells. With BEAS-ACE2 cultivated upon the MatriWell's hydrogel and embedded in lung tissue-specific ECM, a

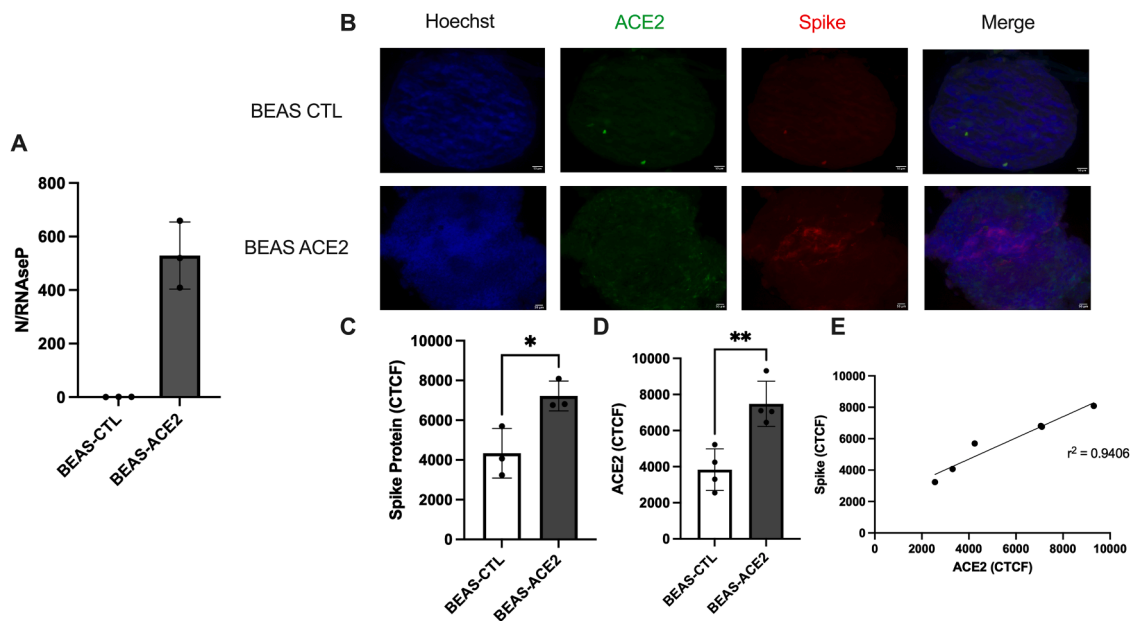


**Fig. 3. Viral load quantification and immunofluorescence assay of BEAS-CTL and BEAS-ACE2 spheroids.** (A) Spheroid intracellular viral concentration. (B) Immunofluorescence microscopy images of the spheroids with nucleus (Hoechst), ACE2, and Spike protein staining. Fluorescence quantification of (C) Spike protein and (D) ACE2 expression. (E) Pearson correlation comparing ACE2 and Spike protein expression. Scale bar: 50  $\mu$ m. \* $p \leq 0.05$ ; \*\* $p \leq 0.01$ .  $n = 3-5$

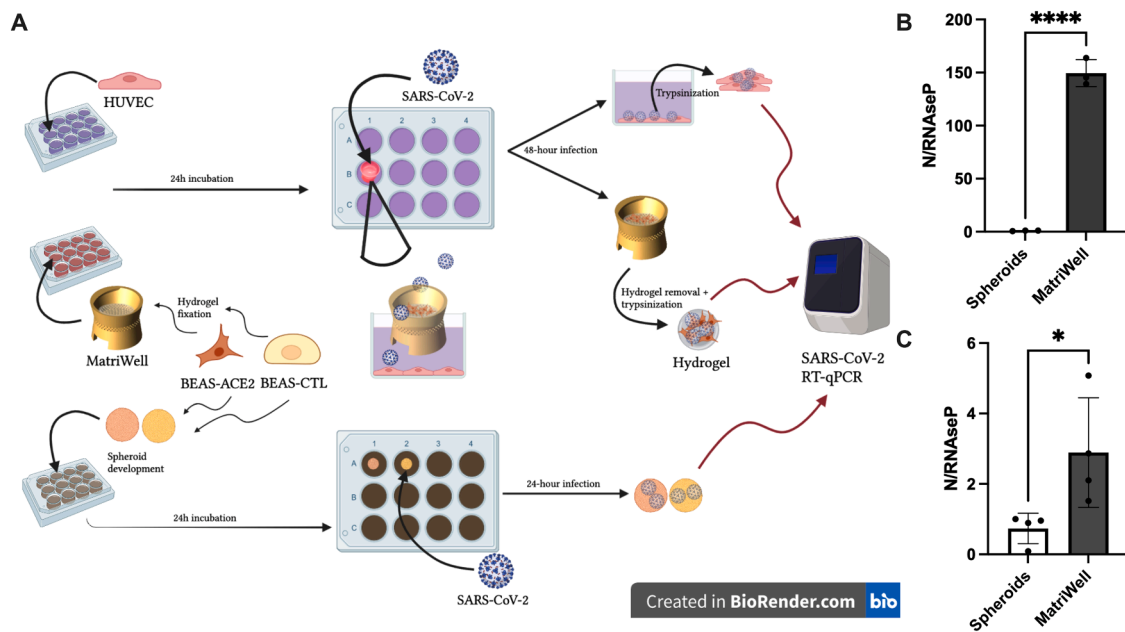


**Fig. 4. SARS-CoV-2 infection of the 3D models.** (A) SARS-CoV-2 infection of spheroids and MatriWells. (B) Comparison of intracellular viral load in BEAS-CTL spheroids and MatriWells. (C) Comparison of intracellular viral load in BEAS-ACE2 spheroids and MatriWells. \*\*\*\* $p \leq 0.0001$ , \* $p \leq 0.05$ .  $n = 5-15$

lung sample had been constructed (Fig. 5A). The lung sample was characterized by a considerable level of accuracy, which stemmed from the interrelation of BEAS-ACE2 cells with each other and with native ECM components. Right beneath the BEAS-ACE2 MatriWells, the HUVEC cells were cultivated on the wells, representing capillaries. SARS-CoV-2 was added to top of the MatriWells where BEAS-ACE2 were seeded (Fig. 4A). The virus infected BEAS-ACE2 and a maximum intracellular viral load was observed 24 hpi (Fig. 5B). SARS-CoV-2 replicated in BEAS-ACE2 and was further released into the HUVEC's supernatant, wherein a viral load of  $1.7 \times 10^4$  PFU/mL was observed 2 hpi, reaching a peak of  $4.7 \times 10^5$  PFU/mL 24 hpi (Fig. 5C). HUVEC cells were also infected by the virus and a maximum viral load, 150-fold higher

compared to 2 hpi ( $p \leq 0.001$ ), was obtained 48hpi (Fig. 5D). These data indicated that SARS-CoV-2 replicated in the cells seeded on the MatriWells and infected HUVEC cells, simulating real viral multiplication in the respiratory system and subsequent hematogenous dissemination.

## Discussion

The respiratory tract, as the first target of SARS-CoV-2, represents a crucial component of viral pathogenesis investigation and validation of therapeutics prior to clinical trials. In this context, careful representation of the lung tissue is necessary for accurate data generation. The development of 3D *in vitro* models that mimic the respiratory tissue

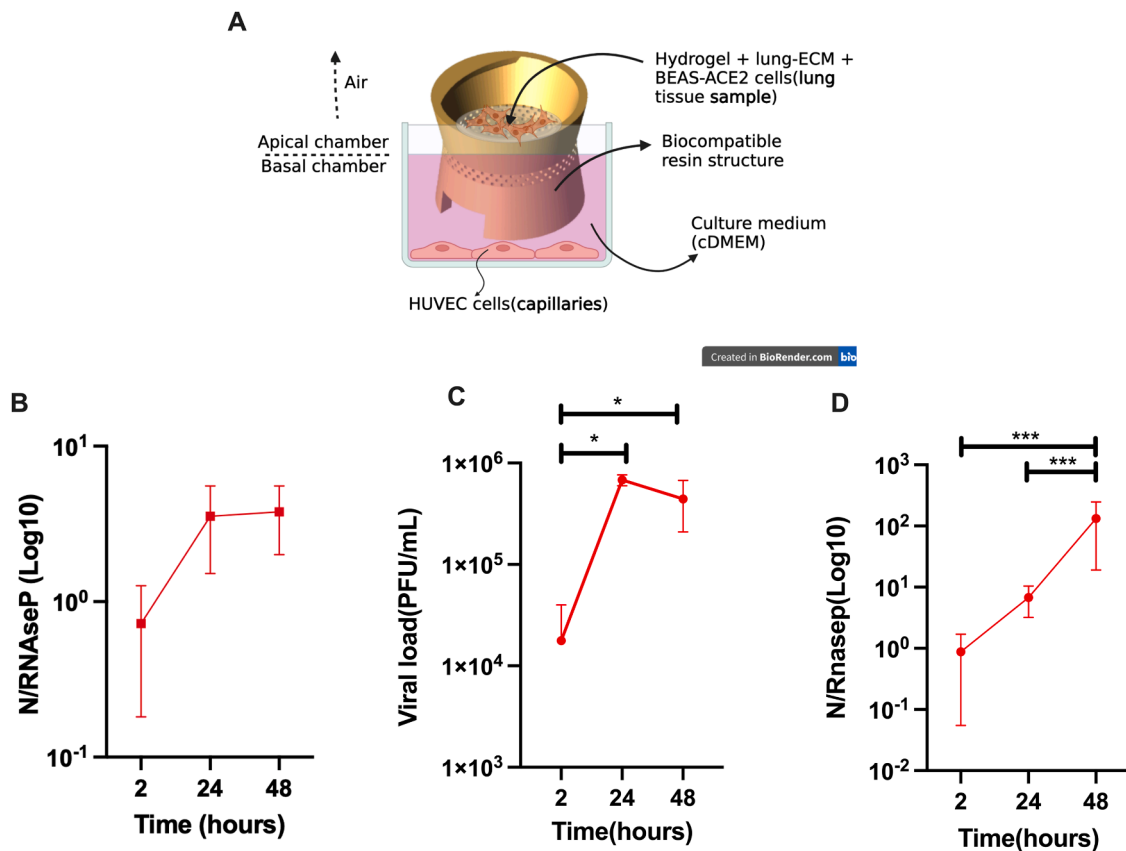


**Fig. 5.** MatriWells representative scheme and SARS-CoV-2 kinetics in BEAS-ACE2 MatriWells and HUVEC cells. (A) Pulmonary ALI creation using the MatriWells, BEAS-ACE2 and HUVEC cells. (B) Intracellular viral load in BEAS-ACE2 MatriWells. (C) Number of viral particles per mL (PFU [plaque-forming units]/mL) in HUVEC's supernatant. (D) Intracellular viral load in HUVEC cells. \* $p \leq 0.05$ ; \*\*\* $p \leq 0.001$ .  $n = 12$ .

constitutes a tailored solution to that goal, which is addressed in this work. Herein, we tested two innovative 3D models to study SARS-CoV-2 replication: spheroids and MatriWells.

The present work is one of the first to use BEAS-ACE2 on these models and pioneers the application of the MatriWells for COVID-19 studies. As previously observed, 2D cultures of bronchial epithelial cell lines do not fully reflect the physiology of the *in vivo* environment [33]. In addition, most of the novel drugs that showed promise in pre-clinical models failed in human trials: half of them due to lack of efficacy and 30% due to toxicity [10]. For those reasons, developing new pre-clinical models as close to the human organism as possible is urgent. The work herein presented addresses that through a process of mimicking the lung tissue by means of 3D culture. We first developed and characterized 3D spheroids of BEAS-2B overexpressing ACE2 using a scaffold-free methodology. Several studies have used BEAS-2B as an *in vitro* cell model of respiratory diseases, including COVID-19 [14,34–36]. However, to the best of our knowledge, the present study was the first to use BEAS-ACE2 3D spheroids in the context of COVID-19.

Our data has shown that the overexpression of ACE2 was associated with an increased size (diameter and volume) of the spheroids. We first hypothesized that this difference would be related to the difference in BEAS-2B and BEAS-ACE2 cell surface areas. However, cells overexpressing ACE2 revealed a smaller area compared to the control group. Indeed, Bolognesi et al. previously demonstrated that the overexpression of proteins interferes with cells' metabolism and size [37], as has our group in prior publications that indicated that BEAS-2B proliferated less after ACE2 overexpression [14]. This contradiction between spheroids' size and cell area could be explained by a deeper analysis of the ACE2 receptor. As a membrane receptor, ACE2, when overexpressed, occupies a significant portion of the cell membrane. Therefore,

the space available for cell-cell interaction is limited. The lesser interaction between cells within a spheroid creates greater space between them, which makes the BEAS-ACE2 spheroid exhibit increased size. In a scenario of low cell-cell interaction, we would expect lower spheroid viability. However, no differences in viability were observed between BEAS-CTL and BEAS-ACE2 spheroids, which indicates that the interaction between cells is not the main factor dictating viability.

Besides influencing cell size, ACE2 also has other important roles. It takes significant part, for instance, in the renin-angiotensin-aldosterone system [RAAS], wherein ACE2 has the potential to increase the levels of Angiotensin 1-7 and decrease the levels of Angiotensin II, favoring cell homeostasis [38] oxidative stress, apoptosis, and cytokine inflammation [39]. Conversely, in the setting of SARS-CoV-2 infection of the spheroids, ACE2 is prejudicial to cells, having been shown to positively influence SARS-CoV-2 entrance and replication in the cells. ACE2, therefore, exerts a dual role in pulmonary cells: it demonstrates a capacity to protect them from death and damage while establishing a state of vulnerability toward viral infection.

This vulnerability placed by ACE2 not only has been confirmed by our spheroid-infected assays, which revealed a higher Spike protein expression in the BEAS-ACE2 group and a strong correlation between ACE2 and Spike protein expression, but also has been previously demonstrated in 2D cultures by our group and several others [14,40,41]. Our group, however, stands out by demonstrating the ability of the virus to infect the spheroids and target the cells in the center using spatial localization by immunofluorescence.

Upon conclusion of the positive influence of ACE2 on SARS-CoV-2 kinetics in spheroids, BEAS-CTL and BEAS-ACE2 cells were employed in the MatriWell. In this model, we were able to create an ALI, in the middle of which the cells were maintained, thus mimicking the

pulmonary environment. Our data on these disruptive models indicated a higher viral load in the MatriWells compared to the spheroids, suggesting more effective viral entry and intracellular replication. The favorable result on the MatriWells could be explained by its protein composition. As a platform derived from the lung's decellularized ECM, the MatriWell likely embodies an intricate assortment of lung ECM proteins, which include fibrous proteins such as collagen and elastin, glycoproteins like fibronectin and laminin, glycosaminoglycans including heparan sulfate and hyaluronic acid, and proteoglycans such as perlecan and versican. The MatriWell's ability to replicate the human ECM positions it favorably for more precise data generation.

In the context of SARS-CoV-2, models that enhance viral kinetics are typically preferred on account of their potential to significantly optimize drug screening processes. When cells that poorly replicate the virus are used for drug screening purposes, they usually mask the effects of the medication being tested. Vero-E6 cells, for instance, due to its ability to extensively replicate SARS-CoV-2, are widely used for SARS-CoV infection studies since 2003 [42]. Additionally, Sasaki et al. also established a clear association between elevated SARS-CoV-2 viral load and elevated quality of models for SARS-CoV-2 investigation in ALI cultures of A549 cells [43]. Hence, considering the favorable SARS-CoV-2 kinetics in the Matriwells, it is possible to state that they are a reliable model for COVID-19 molecular investigation.

The literature had previously established ALI cultures as a highly effective technique for realistic cell morphology and function representation of the *in vivo* airway epithelium [44]. ALI airway models accurately simulate the barrier and metabolic properties of the respiratory epithelium as well as the cellular transcriptional profile of that tissue [45]. In a genetic expression pattern comparison between nasal epithelial cells and cells cultured in ALI models, for example, a similarity of 96% of gene expression between these two groups has been reported [46]. Moreover, these cultures are able to reproduce *in vivo* toxicity responses, including cilia dysfunction [47] and goblet cell hyperplasia [45], which is extremely suitable for a viral infection scenario such as the one presented by this work. In addition to that, at the same time that ALI models have been shown to express considerable levels of genes involved in cell cycle and proliferation [48], previous research has demonstrated that coronavirus infection in the human lung is highly dependent on the differentiation state of airway epithelium [49], which makes these models highly appropriate for coronavirus studies. Specifically in the context of SARS-CoV-2, Sasaki et al. have also observed that ALI cultures, owing to a cell phenotype switch mechanism, renders A549 cells, which are normally resistant to SARS-CoV-2 infection, susceptible to the virus [43]. It is possible to conclude, thus, that ALI models constitute a highly satisfactory technique for SARS-CoV-2 investigation, confirming our previous finding that MatriWells are indeed, in the context of this work, the most reliable model for SARS-CoV-2 infection representation.

Analyzing the viral infection of the MatriWells from an in-depth perspective, we could observe that the concomitant increase in viral load in BEAS-ACE2 and HUVEC cells indicated that SARS-CoV-2 was able to penetrate the hydrogel, reach and replicate in the BEAS-ACE2 cells, exocytose them and reach the endothelial cells, hence appropriately representing viral hematogenous dissemination through the pulmonary ALI. The similar and concomitant increase in viral load in the MatriWells' supernatant validated the aforementioned finding.

Simultaneously, the study of COVID-19 has also been benefited by the investigation and testing of other 3D models. Si L et al., for example, created a microfluidic airway chip (human organ chip) containing specified membranes. The device allows rapid identification of existing approved drugs that could be repurposed for pandemic-virus applications [50]. It is also possible to integrate SARS-CoV-2 genomics with the microfluidic platforms, producing a COVID-19-on-a-chip that has the capacity to screen therapeutics specifically toward the evolving viral variants [51]. Considering the potential of the MatriWells and spheroids to contribute to COVID-19 drug development, both previously

mentioned works are markedly complementary to the present one.

Sun AM et al. have also suggested that lung chips can be incorporated into multi-organ chips, which would enable tracking of extrapulmonary manifestations (such as those in the heart, liver and kidneys) and their association with the lungs, allowing for disease severity analysis [52]. For that reason, the mentioned study would also complement the one herein presented as it has the potential to increment the level of understanding of COVID-19.

Organoids are another relevant model in the context of respiratory diseases study. Derived from stem cells or adult tissues, they are miniaturized *in vitro* organ models that differentiate into the desired cell types. In the context of COVID-19, lung organoids have been applied to monitor viral infection and inspect the pathological damage caused by SARS-CoV-2 [53], which, along with our spheroids, could potentiate the investigation concerning the actual influences of the virus upon the respiratory tissue.

## Conclusion

The present research is an important scientific advancement as it introduces two novel 3D models methods for mimicking lung tissue: spheroids and MatriWells.

Our study revealed that ACE2 overexpression increased the size of the spheroids, even though BEAS-ACE2 cultivated in 2D demonstrated smaller area compared to BEAS-CTL cells. At the same time, ACE2 has been shown to make the spheroids more susceptible to SARS-CoV-2 infection: a strong correlation between ACE2 and Spike protein expression was detected and confirmed by a higher Spike protein expression in the BEAS-ACE2 spheroids.

The MatriWells, in turn, allowed for the creation of a pulmonary ALI, which has been proved by various previous works to be an accurate interface for realistic genetic expression and differentiation of native tissue, pathological damage depiction, and susceptibility to SARS-CoV-2. Viral kinetics in these models revealed a solid representation of viral replication and hematogenous dissemination through the ALI.

Altogether, the present work presents an original and reliable set of models for respiratory diseases investigation, which, along with the data generated on ACE2 influences upon the infection, brings perspective into COVID-19 studies, streamlining the process of drug development for the broad array of respiratory illnesses that pose a threat to the human organism.

## Declaration of Competing Interest

The authors declare that they have no known competing financial interests or personal relationships that could have appeared to influence the work reported in this paper.

Gabriel Romero Liguori and Tácia Tavares Aquinas Liguori are, respectively, the Chief Executive Officer and the Chief Scientific Officer of TissueLabs Sagl (Manno, Switzerland), the company which developed and produced MatriWell cell culture inserts. The remaining authors have no conflict of interest to declare.

## Data Availability

Data will be made available on request.

## Acknowledgements

The authors thank Isabella Bustelli and Danielle Sobral for their technical assistance, Prof. Dr. José Luiz Provença Modena, for kindly providing the SARS-CoV-2 strain used in the experiments, Prof. Mariangela Macchione for kindly providing Human lung epithelial BEAS-2B cells.

## Funding

This work was supported by The São Paulo Research Foundation (FAPESP), grant numbers: 2016/20796-2 (RPU), 2020/04709-8 (RPU), 2020/13480-4 (CMP), 2019/10922-9 (RSS); National Council for Scientific and Technological Development (CNPq), grant number 303035/2018-8 (CMP), Research Foundation of Santa Casa de Sao Paulo School of Medical Sciences grant number 2021/2023.

## Supplementary materials

Supplementary material associated with this article can be found, in the online version, at [doi:10.1016/j.bbiosy.2023.100082](https://doi.org/10.1016/j.bbiosy.2023.100082).

## References

- Cucinotta D, Vanelli M. WHO Declares COVID-19 a Pandemic. *Acta Biomed* 2020; 91:157–60. <https://doi.org/10.23750/abm.v91i1.9397>.
- Coronavirus Resource Center, Johns Hopkins University. <https://coronavirus.jhu.edu/map.html>, 2023 (accessed 01 February 2023).
- Umakanthan S, Sahu P, Ranade AV, Bukelo MM, Rao JS, Abrahao-Machado LF, et al. Origin, transmission, diagnosis and management of coronavirus disease 2019 (COVID-19). *Postgrad Med J* 2020;96:753–8. <https://doi.org/10.1136/postgradmedj-2020-138234>.
- Gibson PG, Qin L, Pua SH. COVID-19 acute respiratory distress syndrome (ARDS): clinical features and differences from typical pre-COVID-19 ARDS. *Med J Aust* 2020;213:54–6. <https://doi.org/10.5694/mja2.50674>. e1.
- Gupta A, Madhavan MV, Sehgal K, Nair N, Mahajan S, Sehrawat TS, et al. Extrapulmonary manifestations of COVID-19. *Nat Med* 2020;26:1017–32. <https://doi.org/10.1038/s41591-020-0968-3>.
- Jackson CB, Farzan M, Chen B, Choe H. Mechanisms of SARS-CoV-2 entry into cells. *Nat Rev Mol Cell Biol* 2022;23:3–20. <https://doi.org/10.1038/s41580-021-00418-x>.
- Brooke GN, Prisch F. Structural and functional modelling of SARS-CoV-2 entry in animal models. *Sci Rep* 2020;10:15917. <https://doi.org/10.1038/s41598-020-72528-z>.
- Barnes PJ, Bonini S, Seeger W, Belvisi MG, Ward B, Holmes A. Barriers to new drug development in respiratory disease. *Eur Respir J* 2015;45:1197–207. <https://doi.org/10.1183/09031936.00007915>.
- Kiener M, Roldan N, Machahua C, Sengupta A, Geiser T, Guenat OT, et al. Human-based advanced in vitro approaches to investigate lung fibrosis and pulmonary effects of COVID-19. *Front Med (Lausanne)* 2021;8:644678. <https://doi.org/10.3389/fmed.2021.644678>.
- Tran BM, Grimley SL, McAuley JL, Hachani A, Earnest L, Wong SL, et al. Air-liquid interface differentiated human nose epithelium: a robust primary tissue culture model of SARS-CoV-2 infection. *Int J Mol Sci* 2022;23. <https://doi.org/10.3390/ijms23020835>.
- Zhao M-M, Yang W-L, Yang F-Y, Zhang L, Huang W-J, Hou W, et al. Cathepsin L plays a key role in SARS-CoV-2 infection in humans and humanized mice and is a promising target for new drug development. *Signal Transduct Target Ther* 2021;6: 134. <https://doi.org/10.1038/s41392-021-00558-8>.
- Colunga Biancatelli RML, Solopov PA, Sharlow ER, Lazo JS, Marik PE, Catravas JD. The SARS-CoV-2 spike protein subunit S1 induces COVID-19-like acute lung injury in K18-hACE2 transgenic mice and barrier dysfunction in human endothelial cells. *Am J Physiol Lung Cell Mol Physiol* 2021;321:L477–84. <https://doi.org/10.1152/ajplung.00223.2021>.
- Krewski D, Acosta D, Andersen M, Anderson H, Bailar JC, Boekelheide K, et al. Toxicity testing in the 21st century: a vision and a strategy. *J Toxicol Environ Health, Part B* 2010;13:51–138. <https://doi.org/10.1080/10937404.2010.483176>.
- Bartolomeo CS, Lemes RMR, Morais RL, Pereria GC, Nunes TA, Costa AJ, et al. SARS-CoV-2 infection and replication kinetics in different human cell types: The role of autophagy, cellular metabolism and ACE2 expression. *Life Sci* 2022;308: 120930. <https://doi.org/10.1016/j.lfs.2022.120930>.
- Jensen C, Teng Y. Is it time to start transitioning from 2D to 3D cell culture? *Front Mol Biosci* 2020;7:33. <https://doi.org/10.3389/fmolb.2020.00033>.
- Habanjar O, Diab-Assaf M, Caldefie-Chezet F, Delort L. 3D cell culture systems: tumor application, advantages, and disadvantages. *Int J Mol Sci* 2021;22. <https://doi.org/10.3390/ijms222212200>.
- Ravi M, Paramesh V, Kaviya SR, Anuradha E, Solomon FDP. 3D cell culture systems: advantages and applications. *J Cell Physiol* 2015;230:16–26. <https://doi.org/10.1002/jcp.24683>.
- Edmondson R, Broglie JJ, Adcock AF, Yang L. Three-dimensional cell culture systems and their applications in drug discovery and cell-based biosensors. *Assay Drug Dev Technol* 2014;12:207–18. <https://doi.org/10.1089/adt.2014.573>.
- Fang Y, Eglen RM. Three-dimensional cell cultures in drug discovery and development. *SLAS Discov* 2017;22:456–72. <https://doi.org/10.1177/1087057117696795>.
- Kronemberger GS, Carneiro FA, Rezende DF, Baptista LS. Spheroids and organoids as humanized 3D scaffold-free engineered tissues for SARS-CoV-2 viral infection and drug screening. *Artif Organs* 2021;45:548–58. <https://doi.org/10.1111/aor.13880>.
- Higashi-Kuwata N, Yabe SG, Fukuda S, Nishida J, Tamura-Nakano M, Hattori S, et al. Generation of Angiotensin-Converting Enzyme 2/Transmembrane Protease Serine 2-Double-Positive Human Induced Pluripotent Stem Cell-Derived Spheroids for Anti-Severe Acute Respiratory Syndrome Coronavirus 2 Drug Evaluation. *Microbiol Spectr* 2022;10. <https://doi.org/10.1128/spectrum.03490-22>.
- Plebani R, Bai H, Si L, Li J, Zhang C, Romano M. 3D Lung Tissue Models for Studies on SARS-CoV-2 Pathophysiology and Therapeutics. *Int J Mol Sci* 2022;23. <https://doi.org/10.3390/ijms231710071>.
- de Melo BAG, Mundim MV, Lemes RMR, Cruz EM, Ribeiro TN, Santiago CF, et al. 3D Bioprinted Neural-Like Tissue as a Platform to Study Neurotropism of Mouse-Adapted SARS-CoV-2. *Adv Biol* 2022;6:e2200002. <https://doi.org/10.1002/adbi.202200002>.
- Zhuang P, Chiang Y-H, Fernanda MS, He M. Using Spheroids as Building Blocks Towards 3D Bioprinting of Tumor Microenvironment. *Int J Bioprint* 2021;7:444. <https://doi.org/10.18063/ijb.v7i4.444>.
- Kim S, Kim EM, Yamamoto M, Park H, Shin H. Engineering multi-cellular spheroids for tissue engineering and regenerative medicine. *Adv Healthc Mater* 2020;9: 2000608. <https://doi.org/10.1002/adhm.202000608>.
- Zhou Y, Horowitz JC, Naba A, Ambalavanan N, Atabai K, Balestrini J, et al. Extracellular matrix in lung development, homeostasis and disease. *Matrix Biol* 2018;73:77–104. <https://doi.org/10.1016/j.matbio.2018.03.005>.
- Kleinman HK, Philip D, Hoffman MP. Role of the extracellular matrix in morphogenesis. *Curr Opin Biotechnol* 2003;14:526–32. <https://doi.org/10.1016/j.copbio.2003.08.002>.
- Frantz C, Stewart KM, Weaver VM. The extracellular matrix at a glance. *J Cell Sci* 2010;123:4195–200. <https://doi.org/10.1242/jcs.023820>.
- Stilhano RS, Samoto VY, Silva LM, Pereira GJ, Erustes AG, Smaili SS, et al. Reduction in skeletal muscle fibrosis of spontaneously hypertensive rats after laceration by microRNA targeting angiotensin II receptor. *PLoS One* 2017;12: e0186719. <https://doi.org/10.1371/journal.pone.0186719>.
- Stuart MP, Matsui RAM, Santos MFS, Cortes I, Azevedo MS, Silva KR, et al. Successful low-cost scaffold-free cartilage tissue engineering using human cartilage progenitor cell spheroids formed by micromolded nonadhesive hydrogel. *Stem Cells Int* 2017;2017:7053465. <https://doi.org/10.1155/2017/7053465>.
- Nasaré AM, Tedesco RC, Cristovam PC, Cenedese MA, Galisteo AJ, Andrade HF, et al. Toxoplasma Gondii infection of chicken embryos causes retinal changes and modulates HSP90B1 gene expression: a promising ocular toxoplasmosis model. *Eur J Microbiol Immunol (Bp)* 2015;5:316–20. <https://doi.org/10.1556/1886.2015.00024>.
- Bergdorf KN, Phifer CJ, Bechard ME, Lee MA, McDonald OG, Lee E, et al. Immunofluorescent staining of cancer spheroids and fine-needle aspiration-derived organoids. *STAR Protoc* 2021;2:100578. <https://doi.org/10.1016/j.xpro.2021.100578>.
- Baarsma HA, Van der Veen CHTJ, Lobebe D, Mones N, Oosterhout E, Cattani-Cavaliere I, et al. Epithelial 3D-spheroids as a tool to study air pollutant-induced lung pathology. *SLAS Discov* 2022;27:185–90. <https://doi.org/10.1016/j.slasd.2022.02.001>.
- Han X, Na T, Wu T, Yuan B-Z. Human lung epithelial BEAS-2B cells exhibit characteristics of mesenchymal stem cells. *PLoS One* 2020;15:e0227174. <https://doi.org/10.1371/journal.pone.0227174>.
- Lemes RMR, Costa AJ, Bartolomeo CS, Bassani TB, Nishino MS, Pereira GJ, da S, et al. 17 $\beta$ -estradiol reduces SARS-CoV-2 infection in vitro. *Physiol Rep* 2021;9: e14707. <https://doi.org/10.14814/phy2.14707>.
- Costa AJ, Lemes RMR, Bartolomeo CS, Nunes TA, Pereira GC, Oliveira RB, et al. Overexpression of estrogen receptor GPER1 and G1 treatment reduces SARS-CoV-2 infection in BEAS-2B bronchial cells. *Mol Cell Endocrinol* 2022;558:111775. <https://doi.org/10.1016/j.mce.2022.111775>.
- Bolognesi B, Lehner B. Reaching the limit. *Elife* 2018;7. <https://doi.org/10.7554/eLife.39804>.
- Seixas MLGA, Mitre LP, Shams S, Lanzuolo GB, Bartolomeo CS, Silva EA, et al. Unraveling muscle impairment associated with COVID-19 and the role of 3D culture in its investigation. *Front Nutr* 2022;9:825629. <https://doi.org/10.3389/fnut.2022.825629>.
- Banu N, Panikar SS, Leal LR, Leal AR. Protective role of ACE2 and its downregulation in SARS-CoV-2 infection leading to macrophage activation syndrome: therapeutic implications. *Life Sci* 2020;256:117905. <https://doi.org/10.1016/j.lfs.2020.117905>.
- Blanco-Melo D, Nilsson-Payant BE, Liu W-C, Uhl S, Hoagland D, Möller R, et al. Imbalanced Host Response to SARS-CoV-2 Drives Development of COVID-19. *Cell* 2020;181:1036–45. <https://doi.org/10.1016/j.cell.2020.04.026>. e9.
- de Vries M, Mohamed AS, Prescott RA, Valero-Jimenez AM, Desvignes L, O'Connor R, et al. A comparative analysis of SARS-CoV-2 antiviral characterizers 3CLpro inhibitor PF-00835231 as a potential new treatment for COVID-19. *J Virol* 2021;95. <https://doi.org/10.1128/JVI.01819-20>.
- Pires De Souza GA, Le Bideau M, Boschi C, Wurtz N, Colson P, Aherfi S, et al. Choosing a cellular model to study SARS-CoV-2. *Front Cell Infect Microbiol* 2022; 12:1003608. <https://doi.org/10.3389/fcimb.2022.1003608>.
- Sasaki M, Kishimoto M, Itakura Y, Tabata K, Intaruck K, Uemura K, et al. Air-liquid interphase culture confers SARS-CoV-2 susceptibility to A549 alveolar epithelial cells. *Biochem Biophys Res Commun* 2021;577:146–51. <https://doi.org/10.1016/j.bbrc.2021.09.015>.
- Chandrasekaran A, Kouthouridis S, Lee W, Lin N, Ma Z, Turner MJ, et al. Magnetic microboats for floating, stiffness tunable, air-liquid interface epithelial cultures. *Lab Chip* 2019;19:2786–98. <https://doi.org/10.1039/C9LC00267G>.
- Cao X, Coyle JP, Xiong R, Wang Y, Heflich RH, Ren B, et al. Invited review: human air-liquid-interface organotypic airway tissue models derived from primary

- tracheobronchial epithelial cells—overview and perspectives. *In Vitro Cell Dev Biol Anim* 2021;57:104–32. <https://doi.org/10.1007/s11626-020-00517-7>.
- [46] Ghosh B, Park B, Bhowmik D, Nishida K, Lauver M, Putcha N, et al. Strong correlation between air-liquid interface cultures and in vivo transcriptomics of nasal brush biopsy. *Am J Physiol-Lung Cell Mol Physiol* 2020;318:L1056–62. <https://doi.org/10.1152/ajplung.00050.2020>.
- [47] Brekman A, Walters MS, Tilley AE, Crystal RG. FOXJ1 Prevents Cilia growth inhibition by cigarette smoke in human airway epithelium *in vitro*. *Am J Respir Cell Mol Biol* 2014;51:688–700. <https://doi.org/10.1165/rcmb.2013-0363OC>.
- [48] Pezzulo AA, Stamer TD, Scheetz TE, Traver GL, Tilley AE, Harvey B-G, et al. The air-liquid interface and use of primary cell cultures are important to recapitulate the transcriptional profile of in vivo airway epithelia. *Am J Physiol Lung Cell Mol Physiol* 2011;300:L25–31. <https://doi.org/10.1152/ajplung.00256.2010>.
- [49] Jia HP, Look DC, Shi L, Hickey M, Pewe L, Netland J, et al. ACE2 receptor expression and severe acute respiratory syndrome coronavirus infection depend on differentiation of human airway epithelia. *J Virol* 2005;79:14614–21. <https://doi.org/10.1128/JVI.79.23.14614-14621.2005>.
- [50] Si L, Bai H, Rodas M, Cao W, Oh CY, Jiang A, et al. A human-airway-on-a-chip for the rapid identification of candidate antiviral therapeutics and prophylactics. *Nat Biomed Eng* 2021;5:815–29. <https://doi.org/10.1038/s41551-021-00718-9>.
- [51] Satta S, Shahabipour F, Gao W, Lentz SR, Perlman S, Ashammakhi N, et al. Engineering viral genomics and nano-liposomes in microfluidic platforms for patient-specific analysis of SARS-CoV-2 variants. *Theranostics* 2022;12:4779–90. <https://doi.org/10.7150/thno.72339>.
- [52] Sun AM, Hoffman T, Luu BQ, Ashammakhi N, Li S. Application of lung microphysiological systems to COVID-19 modeling and drug discovery: a review. *Biodes Manuf* 2021;4:757–75. <https://doi.org/10.1007/s42242-021-00136-5>.
- [53] Han Y, Yang L, Lacko LA, Chen S. Human organoid models to study SARS-CoV-2 infection. *Nat Methods* 2022;19:418–28. <https://doi.org/10.1038/s41592-022-01453-y>.